

## Influence of Cellulose Nanofibers on the Morphology and Physical Properties of Poly(lactic acid) Foaming by Supercritical Carbon Dioxide

Se Youn Cho, Hyun Ho Park, Young Soo Yun, and Hyoung-Joon Jin\*

Department of Polymer Science and Engineering, Inha University, Incheon 402-751, Korea

Received March 20, 2012; Revised July 3, 2012; Accepted July 4, 2012

**Abstract:** The foaming process of poly(lactic acid) (PLA)/cellulose nanofiber (CNF) nanocomposites using supercritical CO<sub>2</sub> as a foaming agent was studied with various CNF contents. CNFs were obtained by sonication, and their morphology was examined by transmission electron microscopy. According to the CNF content, the changes in the rheological and the thermal properties of the nanocomposites were studied through viscometry and differential scanning calorimetry. The viscosity of the composites increased with increasing CNF content. The effects of the CNF content on the foam properties and morphologies were evaluated. Compared to neat PLA foam, the PLA/CNF nanocomposite foams exhibited decreased cell size as well as increased cell density and foam density due to the improved viscous properties.

**Keywords:** poly(lactic acid), cellulose nanofiber, nanocomposites, rheological properties, foam processing.

### Introduction

Considerable effort has recently been directed at developing bio-based replacements for petroleum-based synthetic plastics. Poly(lactic acid) (PLA), a linear aliphatic thermoplastic obtained from the ring-opening polymerization of lactide, is one of the most popular bio-based polymers due to its reasonable physical and mechanical properties comparable to those of other synthetic plastics.<sup>1</sup> Extensive research has been conducted for novel applications with short lifecycle, such as biomedical applications, packaging, and agricultural materials.<sup>2</sup>

With the associated environmental benefits, the polymer foam process using supercritical CO<sub>2</sub> is a promising process for large volume packaging applications or high added-value products, such as biomedical implants.<sup>3,4</sup> Although some controversy remains over the polymer foam process and phenomena, good diffusion of the gas blowing agent into the polymer is required, and nucleation and growth of pores are performed under cooling conditions and polymer viscosity. Because of its good ability to dissolve CO<sub>2</sub>, PLA is a good candidate for foaming with supercritical CO<sub>2</sub> to form a cellular matrix. However, PLA suffers the disadvantages of low melt strength and susceptibility to hydrolytic degradation, which may result in deterioration of the rheological properties and may limit the blow molding and foaming abilities.<sup>5,6</sup> To overcome these shortcomings, diverse efforts have been reported for controlling the melt rheology of PLA by increasing molecular weight using branching<sup>7</sup> or chain

extending.<sup>5</sup> Other approaches are the incorporation of organic/inorganic fillers which improve the mechanical properties or raising the cellular densities through heterogeneous bubble nucleation by adding reinforcing fillers.<sup>8,9</sup> Among suitable reinforcing materials, natural fillers, such as microcrystalline cellulose, wood flour, or wood fibers, have attracted attention due to their full bio-composites.<sup>10,11</sup>

Cellulose nanofiber (CNF), a 'green' nano-sized material, is a suitable reinforcing agent for nanocomposite applications due to its exceptional high specific strength and modulus, low density, chemical tunability, renewable nature, and relatively low cost.<sup>12-14</sup> However, CNFs are still used in a limited industrial extent associated with low dispersibility in a polymer matrix and low thermal stability. The large hydroxyl groups of the nanocrystal surface and the nonpolar characteristics of most thermoplastics hinder acceptable dispersion levels of the nanofiller in the matrix, which produces inefficient composites.

In this research, we studied the processing and properties of PLA/CNF nanocomposites and their foams prepared by pressure quenching of supercritical CO<sub>2</sub>. The CNFs underwent surface modification to enhance the affinity between the two polymers. The effects of small additions of CNFs on the thermal, rheological, and foaming behaviors of the PLA-based composites were investigated in terms of the cell morphology and foam density of the PLA.

### Experimental

**Materials.** PLA, grade 2002D was purchased from Nature

\*Corresponding Author. E-mail: hjjin@inha.ac.kr

Works (USA). The microcrystalline cellulose powder was purchased from Sigma-Aldrich.

**Preparation of CNFs.** Ten grams of microcrystalline cellulose powder was added to 200 mL of deionized (DI) water. After sonication in a bath for 24 h using an ultrasonic generator (Kyungill Ultrasonic Co., Korea), 1 L of DI water was added and allowed to stand for 24 h. The supernatant of the suspension was separated and centrifuged for 20 min at 5,000 rpm. The obtained CNFs were re-dispersed in DI water and sonicated for 1 h at ambient temperature.

**Surface Modification of CNFs.** The CNF surface was modified according to a previously reported procedure.<sup>15</sup> Briefly, CNFs in aqueous suspension (100 mg/mL) were solvent exchanged to acetone and then to dry toluene. CNFs were placed in a 500 mL beaker containing a mixture of 108 g of toluene, 105 g of acetic acid, and 0.5 mL of 70% perchloric acid. After vigorous stirring for 1 min, 54 g of acetic anhydride was added, and the mixture was stirred vigorously for 1 min. The mixture was allowed to stand for 1 h at room temperature. After the reaction, the modified CNFs were washed thoroughly 3 times with methanol and were then washed 3 times with DI water.

**Preparation of PLA/CNFs Nanocomposites.** PLA/CNF nanocomposites were prepared using a solvent mixture followed by hot pressing. The nanocrystals in aqueous medium were solvent-exchanged to acetone and then to chloroform by centrifuging and re-dispersing steps. To measure the CNF concentration, a small amount of the CNFs in chloroform was cast in a glass dish and allowed to evaporate. The CNFs suspended in chloroform were stirred, and PLA was gradually added to the suspension at 55 °C. The CNF weight content was kept at 1, 2, and 5 wt%. The mixture was cast and allowed to evaporate by oven vacuum drying at 55 °C for 3 days. After being crushed into small pieces, the composite films were obtained by hot pressing at 200 °C for further characterization. Neat PLA was processed in the same way.

**Foam Processing of PLA/CNFs Nanocomposites.** Physical foaming was conducted in a high-pressure stainless steel autoclave. Round plate samples of neat PLA and PLA/CNF nanocomposites were prepared using a compression mold with a diameter of 10 mm and thickness of 1 mm. After weighing, each sample was placed on a sample holder inside the autoclave. The autoclave was filled with a blowing agent, compressed CO<sub>2</sub>, for a few seconds and then pressurized with the blowing agent and heated to the solubilization temperature. The pressure of the blowing agent at this temperature was adjusted to the desired saturation pressure (20 MPa). A solubilization time of about 1 h was maintained to ensure equilibrium. After saturation, the pressure was quenched to atmospheric pressure within 3 s, and the samples were taken out. The foam structure was allowed to grow fully during rapid depressurization.

**Characterization.** Transmission electron microscopy (TEM, CM200, Philips, Netherlands) was used to examine the mor-

phology of the CNFs. Fourier transformed infrared spectroscopy (FTIR, VERTEX 80v, Bruker Optics, Germany) was used to study the structures of the modified CNFs. Differential scanning calorimetry (DSC, Perkin Elmer Jade) was used to investigate the thermal properties of the PLA/CNF nanocomposites. The viscosities were measured using a Brookfield DV-II+pro viscometer (Brookfield Engineering Laboratories Ltd., Middleboro, MA). Foam morphology, cell size, and average cell density were characterized using field emission scanning electron microscopy (FESEM, S-4300SE, Hitachi, Japan) at an accelerating voltage of 15 kV. The number of cells in a cross-field and their size were determined using image J (National Institutes of Health, USA), based on SEM micrographs. At least 50 cells in each SEM micrograph were measured. The cell density ( $N_c$ ) was calculated according to eq. (1):<sup>5</sup>

$$N_c \approx 10^4 [1 - (\rho_f / \rho_p)] / d^3 \quad (1)$$

where  $\rho_p$  is the density of the polymer matrix,  $\rho_f$  is the density of the foam, and  $d$  is the mean cell size in millimeters.

## Results and Discussion

CNFs are commonly prepared from native semicrystalline cellulose by using sulfuric acid hydrolysis, which breaks down the cellulose into elementary crystalline domains by removing the amorphous cellulose segments. However, strong acid treatment introduces sulfate groups onto the surface of the CNFs and rapidly decreases their degree of polymerization.<sup>16,17</sup> Consequently, the degradation temperatures are considerably decreased compared to native cellulose, and this reduction of thermal stability interrupts their use in the typical processes of producing composites with thermoplastics. In this study, we prepared CNFs by ultra-sonication followed by centrifugation to avoid any degradation of thermal properties. As shown in Figure 1, extended ultra-sonication treatment allowed the creation of fragments from the microcrystalline cellulose. Among these shreds, the small fragments could disperse and float in water. The CNFs were acquired by separation of these floating materials. TEM images of the CNFs produced by sonication are shown in Figure 2. The CNFs seemed to be almost the same size as the cotton-based cellulose nanofibers reported in other studies, with a length of several micrometers and a width of less than 10 nm.<sup>18</sup> However, the boundaries of the CNFs are unclear in the TEM images due to the limited hydrolysis of the cellulose amorphous region compared to an acid treatment.

To obtain homogeneous mixing of the hydrophilic natural filler and hydrophobic polymer matrix, the hydroxyl groups on the CNF surface were modified through esterification. The modification of the CNFs was monitored by FTIR analysis. In Figure 3(b), the IR spectra of the acetylated CNFs showed a significant decrease in the O-H band (3338 cm<sup>-1</sup>)

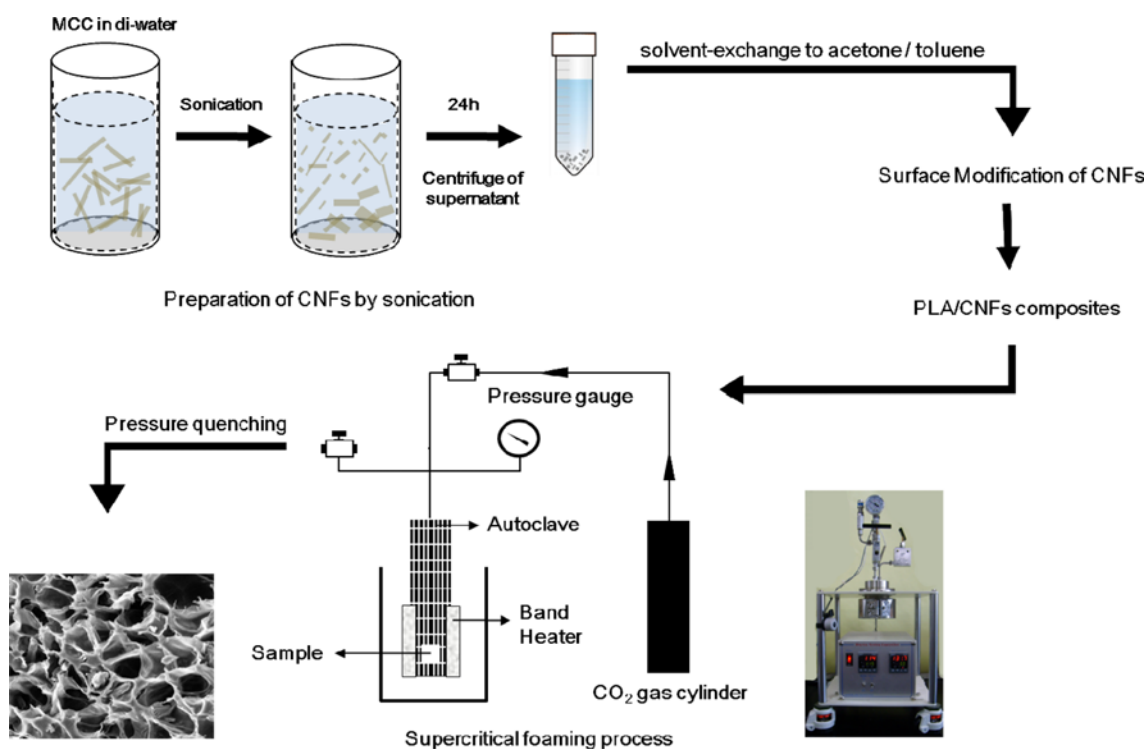


Figure 1. Schematic illustration of PLA/CNF nanocomposite and foaming process.

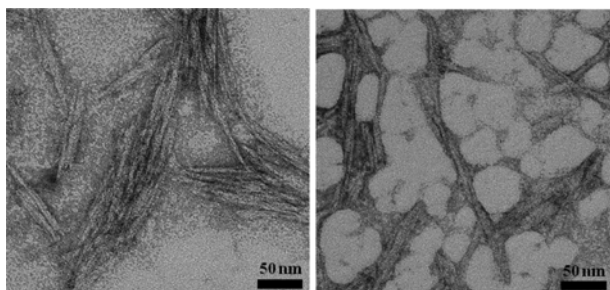


Figure 2. TEM image of CNFs prepared by sonication.

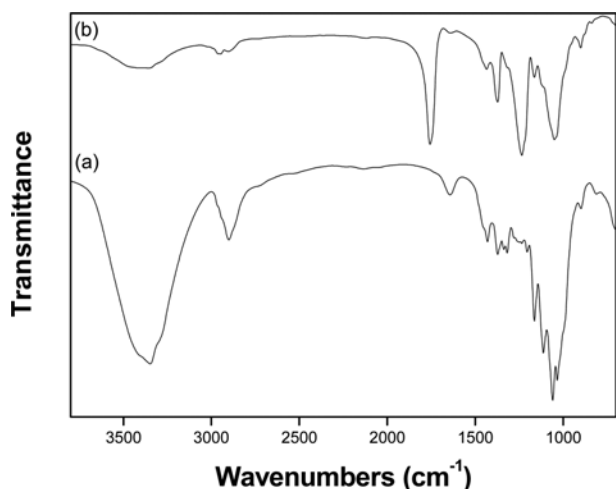


Figure 3. FTIR spectra of (a) CNFs and (b) modified CNFs obtained by sonication treatment.

as a result of esterification and increases in the three major bands of cellulose triacetate: the C=O ( $1740\text{ cm}^{-1}$ ), C-O ( $1231\text{ cm}^{-1}$ ), and C-CH<sub>3</sub> ( $1371\text{ cm}^{-1}$ ) bands.<sup>19</sup> These analyses confirmed a decrease in the number of hydrophilic hydroxyl groups, which may have facilitated the good adhesion of the CNFs with the polymer matrix.

DSC thermograms were used to investigate the thermal properties of the PLA/CNF nanocomposites, and the resulting DSC data are arranged in Table I. The results indicated that the addition of CNFs, in all composite types, did not significantly affect the glass transition and melting behavior of PLA. However, the CNF content influenced the melt crystallization temperatures ( $T_{mc}$ ), which were slightly lower than that of neat PLA because of the nucleating effect of the well-dispersed CNFs. The strong interaction between the polymer matrix and the nano-fillers immobilized and hindered the mobility of the PLA molecules and promoted their

Table I. DSC Data Recorded for PLA/CNF Nanocomposites: Glass Transition Temperature ( $T_g$ ), Melt Crystallization Temperature ( $T_{mc}$ ), Melting Temperature ( $T_m$ ), and Degree of Crystallinity ( $X_c$ )

CNFs Content (wt%)	$T_g$	$T_{mc}$	$T_m$	$X_c$
0	59.6	116.2	166.3	21.3
1	59.9	115.3	165.1	35.6
3	59.4	114.9	165.9	42.6
5	60.2	115.2	166.1	43.1

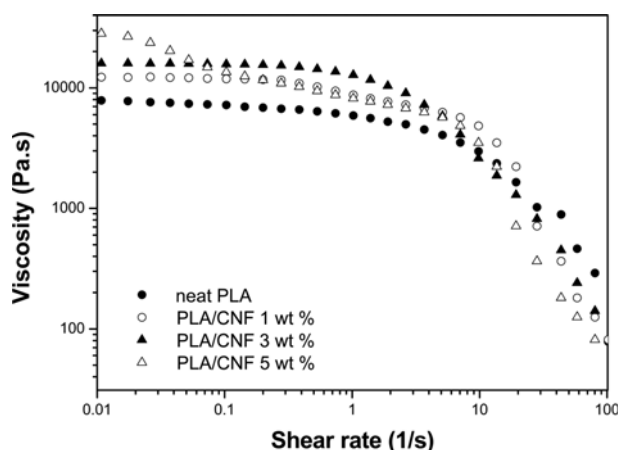


**Figure 4.** Complex viscosity curves for neat PLA and PLA/CNF nanocomposites.

crystallization.<sup>20</sup> Accordingly, CNFs in the composites can serve as a crystal nucleating interface to increase the crystallinity from 21% to around 40%. A value of 93 J/g was used as the theoretical heat of fusion of the PLA.<sup>21</sup> The highest CNF content (5 wt%) showed higher  $T_{mc}$  because the excessive number of interacting sites reduced the mobility of the PLA molecules. Additionally, the CNF aggregates may have physically hindered the crystallization process.

In the polymer foaming process, the melt viscosity is an important parameter for the cell nucleation rate, the growth of nuclei, and the stabilization of the foamed cellular structure. However, due to their linear structure and high rigidity, PLA chains cannot entangle as rapidly as typical foaming materials can, and they show a low melt strength that decreases the foam stabilization. The effect of filler addition on the rheological properties was investigated on the basis of dynamic oscillatory shear measurements, and the resulting viscosity curves are shown in Figure 4. The complex viscosity of neat PLA exhibited typical Newtonian behavior in the low shear rate region and shear thinning commenced up to around  $10 \text{ s}^{-1}$ . The complex viscosity of the CNF-incorporated nanocomposites was higher overall than that of neat PLA and increased with increasing CNF content. At a filler content of 1 and 2 wt%, similar Newtonian behavior with much higher complex viscosity was observed. A literature review suggested that the high viscosities of the polymer matrix with nanometric cellulose fillers are attributable to filler-filler interactions through hydrogen bonding and a good filler-matrix interfacial interaction. Consequently, the flow restrictions of the PLA chains result from the strong interaction between the modified CNFs and the PLA molecules, which enhances the melt viscosity of the PLA/CNF nanocomposites. However, the viscosity of the PLA/CNF (5 wt%) nanocomposite decreased rapidly even from the highest initial viscosity, which may have been caused by the tendency of the CNFs at high content to agglomerate into larger aggregates and induce a

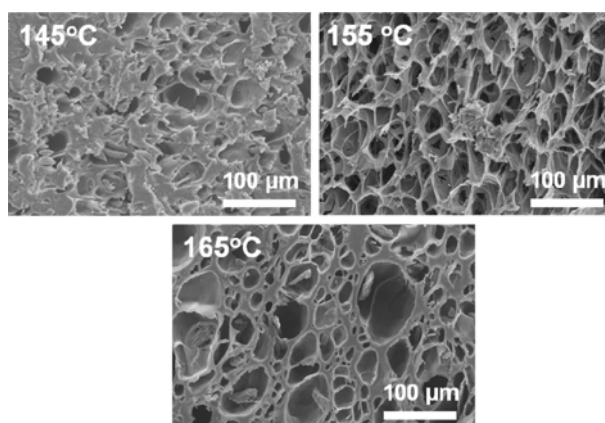


**Figure 5.** Effect of foaming temperature on cell morphology (neat PLA, 20 MPa).

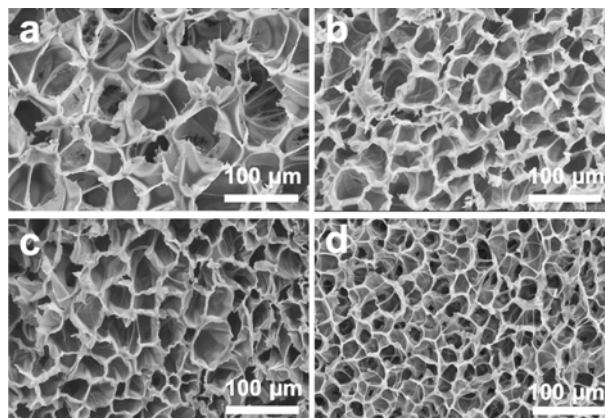


**Figure 6.** Effect of CNF content on cell morphology (20 MPa, 155 °C): (a) neat PLA, and (b) 1, (c) 2, and (d) 5 wt% CNFs.

plasticizer behavior.

Figure 5 shows the effect of the processing temperature ranging from 145 to 165 °C on the cellular structure of the PLA foamed samples. A few cellular structures were formed owing to the unsaturated foaming temperature (145 °C). A collapsed cellular structure was observed at 165 °C because the melt viscosity was too low for stabilization of the foamed structure, which was due to the lowered melt temperature of PLA by dissolution of  $\text{CO}_2$  gas.<sup>22</sup>

Differences in the cellular morphology of neat PLA and the three PLA/CNF composites are shown in Figure 6. The SEM images revealed well interconnected foams of PLA nanocomposites. Neat PLA exhibited cellular structures with large cell diameters of  $52.6 \mu\text{m}$  and a cell density of  $0.56 \times 10^9 \text{ cells/cm}^3$ . As shown in Table II, the average cell size of the PLA foams decreased with increasing CNF content due to the increased viscosity which obstructed cell growth in the polymer matrix. The solubility and diffusivity of gas in semi-crystalline polymers influence the degree of crystallinity because gas does not dissolve in the crystallites. Increasing the mass fraction of crystallite in the polymer

**Table II. Foam Characteristics of PLA/CNF Nanocomposites**

CNFs Content (wt%)	Cell Size ( $\mu\text{m}$ )	Average Cell Density ( $10^8\text{cells}/\text{cm}^3$ )	Foam Density ( $\text{g}/\text{cm}^3$ )
0	52.6	0.56	0.23
1	37.3	1.21	0.15
2	32.9	2.45	0.16
5	26.7	4.21	0.25

reduces the amorphous matrix mass fraction. Consequently, the incorporation of CNFs affected the rheological properties and the crystallinity of the PLA/CNF nanocomposites, which led the different cellular morphology of the PLA foams.

The bulk foam densities were measured, and the results are presented in Table II. Foam density of neat PLA was higher than that of the nanocomposites with 1 and 3 wt% of CNFs owing to its weak melt strength to resist the cell expansion. On the other hand, the cell structures of the nanocomposite with 5 wt% of CNFs foams exhibited the highest foam density, which might be due to the redundant nucleation site.

## Conclusions

PLA polymer nanocomposites with added CNF were prepared by solvent mixture followed by hot pressing. The surface modification of the nanocomposites was attributed to the enhanced interaction between the CNFs and the PLA molecules. As a nano-sized filler, the CNFs acted as nucleating agents at low content, and as the CNF content increased, they began to physically hinder the chain mobility of the PLA. Dynamic rheological studies showed that the PLA/CNF nanocomposites had higher viscosity than pure PLA did. Neat PLA and PLA/CNF nanocomposites were then foamed by using a mixture of  $\text{CO}_2$  as a blowing agent in a foaming process. Compared to the neat PLA foam, the PLA/CNF nanocomposite foams exhibited decreased cell size as well as increased cell density and foam density due to the improved viscous properties. By controlling the nanometric filler and processing conditions, PLA nanocomposite foams with different cellular structures could be obtained for various applications.

**Acknowledgment.** This study was supported by INHA UNIVERSITY Research Grant (2013).

## References

- (1) L. T. Lim, R. Auras, and M. Rubino, *Prog. Polym. Sci.*, **33**, 820 (2008).
- (2) Y. M. Corre, A. Maazouz, J. Duchet, and J. Reigner, *J. Supercrit. Fluid*, **58**, 177 (2011).
- (3) Z. Zhang and Y. P. Handa, *Macromolecules*, **30**, 8505 (1997).
- (4) L. Yu, H. Liu, K. Dean, and L. Chen, *J. Polym. Sci. Part B: Polym. Phys.*, **46**, 2630 (2008).
- (5) Y. Di, S. Iannace, E. D. Maio, and L. Nicolais, *Macromol. Mater. Eng.*, **290**, 1083 (2005).
- (6) R. Rizvi, B. Cochrane, H. Naguib, and P. C. Lee, *J. Cell. Plast.*, **47**, 283 (2011).
- (7) J. Nangeroni and J. Randall, WO Patent WO/2009/134688 (2009).
- (8) S. S. Ray and M. Okamoto, *Macromol. Mater. Eng.*, **288**, 936 (2003).
- (9) M. A. Huneault and H. Li, *Polymer*, **48**, 270 (2007).
- (10) M. S. Huda, L. T. Drzal, M. Misra, and A. K. Mohanty, *J. Appl. Polym. Sci.*, **102**, 4856 (2006).
- (11) L. M. Matuana and O. Faruk, *Express Polym. Lett.*, **49**, 621 (2010).
- (12) Y. Habibi, L. A. Lucia, and O. J. Rojas, *Chem. Rev.*, **110**, 3479 (2010).
- (13) A. C. W. Leung, S. Hrapovic, E. Lam, Y. Liu, K. B. Male, K. A. Mahmoud, and J. H. T. Luong, *Small*, **7**, 302 (2011).
- (14) O. V. D. Berg, J. R. Capadona, and C. Weder, *Biomacromolecules*, **8**, 1353 (2007).
- (15) D. Y. Kim, Y. Nishiyama, and S. Kuga, *Cellulose*, **9**, 361 (2002).
- (16) M. Roman and W. T. Winter, *Biomacromolecules*, **5**, 1671 (2004).
- (17) H. Håkansson and P. Ahlgren, *Cellulose*, **12**, 177 (2005).
- (18) F. Hurtubise, *Tappi J.*, **45**, 460 (1962).
- (19) Y. Di, S. Iannace, E. D. Maio, and L. Nicolais, *J. Polym. Sci. Part B: Polym. Phys.*, **43**, 689 (2005).
- (20) E. Fischer, H. J. Sterzel, and G. Wegner, *Colloid Polym. Sci.*, **251**, 980 (1973).
- (21) Y. Habibi, A. L. Goffin, N. Schiltz, E. Duquesne, P. Dubois, and A. Dufresne, *J. Mater. Chem.*, **18**, 5002 (2008).
- (22) L. M. Matuana and C. A. Diaz, *Ind. Eng. Chem. Res.*, **49**, 2186 (2010).